Strange stars admixed with dark matter: equiparticle model in a two fluid approach

Isabella Marzola, Éverson H. Rodrigues, Anderson F. Coelho, and Odilon Lourenço

Departamento de Física e Laboratório de Computação Científica Avançada e Modelamento (Lab-CCAM),
Instituto Tecnológico de Aeronáutica, DCTA, 12228-900, São José dos Campos, SP, Brazil

(Dated: September 20, 2024)

In this work we explore the possible scenario of strange stars admixed with fermionic or bosonic dark matter. For the description of the "visible" sector, we use a specific phenomenological quark model that takes into account in-medium effects for the quark masses through a suitable baryonic density dependence, in which the free parameters are chosen from the analysis of the stellar matter stability window (parametrizations presenting lower energy per baryon than iron nuclei). In the case of the dark sector, we investigate the predictions of fermionic and bosonic models. In the former we consider a spin 1/2 dark particle, and the latter is described by a dark scalar meson. Both models present a repulsive vector interaction, particularly important for the bosonic model since it helps avoiding the collapse of the star due to the lack of the degeneracy pressure. Our results point out to possible stable strange stars configurations in agreement with data from PSR J0030+0451, PSR J0740+6620, NICER and HESS J1731-347. As another feature, we find stars with dark matter halo configurations for lower values of the dark particle mass.

I. INTRODUCTION

Stars are some of the most studied astrophysical systems in the universe. The detailed composition of these compact objects, as well as their structure and dynamics, are still not completely understood by astrophysicists and, for decades, it has been subject of intense research encompassing many areas of physics such as thermodynamics, quantum field theory, general relativity, and nuclear reactions, for instance. Features of the strongly interacting matter can also be investigated due to the extreme conditions present in the core of the stars, region expected to be at very high density regime. The input used to correctly describe the compressed stellar matter (CSM) comes from models where hadrons (baryons and mesons) are the proper degrees of freedom. Nevertheless, there is also another branch of study that considers quarks as the building blocks in models from which equations of state are derived and applied to the CSM formulation. This approach is based on the quark stars hypothesis proposed long time ago in [1, 2], and later on supported by Bodmer [3] and Witten [4] who established the so called Bodmer-Witten conjecture: quark matter consisting of u, d, and s quarks in beta equilibrium can present lower energy per baryon than hadronic matter. Evidences for quark matter composition in cores of massive stars were recently discussed in Refs. [5, 6].

Both hadronic and phenomenological quark models, constructed for the aforementioned purpose, can be tested against a large number of new astrophysical observational measurements, recently emerged due to (i) the detection of gravitational waves, coming from a binary system with its respective electromagnetic counterparts [7], made by the LIGO and Virgo Collaboration [8–10], (ii) the data concerning the massive millisecond pulsars PSR J0030+0451 [11, 12] and PSR J0740+6620 [13, 14], provided by the NASA's Neutron star Interior Composition Explorer (NICER) x-ray telescope based on the International Space Station [15], and (iii) the first simultaneous measurements of mass, radius, and surface temperature of the HESS J1731-347 compact star [16].

Recently many researchers have been dedicated efforts to better comprehend the physics of these objects, that may present another mysterious component as well, named as dark matter (DM) [17–19]. The main evidences for the existence of non-luminous matter come from the analysis of galaxies rotation curves, and from the use of gravitational lensing methods [20, 21], that lead to visible galaxy clusters masses of around 10% to 20%, being the remaining mass due to DM. Measurements of the anisotropy of cosmic microwave background also suggest presence of DM [22–27]. It is a consensus that the universe, as we know nowadays, is 27% composed by DM, 68% of dark energy, and 5% of ordinary matter.

In this work we study the possibility of existence of strange stars admixed with fermionic and bosonic dark matter, in agreement with the astrophysical constraints mentioned before, by using a particular effective quark model in the "visible" sector, the equiparticle (EQP) model in our case, in which constituent quark masses ($m_{u,d,s}$) are medium dependent, more specifically density dependent in the case of stellar matter at $T = 0$. Temperature effects on $m_{u,d,s}$ can be found in [28–31], and in [32], modified density dependencies of these quantities are proposed. The thermodynamical inconsistency of the original model was solved in [33] through a suitable connection between the quark Fermi momentum and the respective effective chemical potential. In [34], some of us have improved this model in order to take into account deconfinement effects through the introduction of the traced Polyakov loop as the order parameter of the confinement/deconfinement first order phase transition. Such a formulation was called PEQM model.

Here we adopt the perspective of the two fluid approach, that only considers gravitational interaction between DM and quark matter. The calculations and results coming from this investigation, all of them in units of $\hbar = c = G = 1$, are organized in this paper as fol-

lows. In Sec. II we present the main quantities related to effective EQP model, and establish the conditions for the physical stability window. In Sec. III we detail the main equations of sate used for the dark sector of our analysis, describing the fermionic and bosonic DM models. Results related to strange stars obtained from this formalism are shown to the reader in Sec. IV. Finally, our final remarks are given in Sec. V.

II. EQUIPARTICLE MODEL

A. Formalism

The EQP model was proposed in [33] as a baryonic density (ρ_b) and temperature (T) dependent model. However, here we focus on the zero temperature regime, as done in [35] and [34], for the study of cold quark stars. For this reason, the formalism of the model will be presented for this case. For a infinitely large system composed by up (u), down (d) and strange (s) quarks, the equations of state are obtained from fundamental thermodynamical relations. For the pressure we have

$$P = -\Omega_0 + \rho_b \frac{\partial m_I}{\partial \rho_b} \frac{\partial \Omega_0}{\partial m_I}, \tag{1}$$

where m_I is the density dependent quark mass term. The energy density reads

$$\mathcal{E} = \Omega_0 - \sum_i \mu_i^* \frac{\partial \Omega_0}{\partial \mu_i^*}, \tag{2}$$

in which μ_i^* is the effective chemical potential that is introduced through the Fermi momentum ($k_{Fi} = \sqrt{\mu_i^{*2} - m_i^2}$) in order to ensure the thermodynamic consistency, as explained in [36], and m_i is the constituent quark mass ($i = u, d, s$). Furthermore, it is possible to obtain the real chemical potentials of the system by the relationship

$$\mu_i = \mu_i^* + \frac{1}{3} \frac{\partial m_I}{\partial \rho_b} \frac{\partial \Omega_0}{\partial m_I}. \tag{3}$$

For all equations presented, the quantity identified as Ω_0, that is responsible for the free system particle contribution, is given by [37],

$$\Omega_0 = \\ -\sum_i \frac{\gamma}{24\pi^2} \left[\mu_i^* k_{Fi} \left(k_{Fi}^2 - \frac{3}{2} m_i^2 \right) + \frac{3}{2} m_i^4 \ln \frac{\mu_i^* + k_{Fi}}{m_i} \right], \tag{4}$$

with $\gamma = 6 = 3$ (color) $\times 2$ (spin) being the degeneracy factor. Concerning the grand-canonical thermodynamic potential, it can be obtained as $\Omega = -P$.

In order to fully describe the model, it is also important to introduce the relations between quark densities (ρ_i)

and other quantities, such as the Fermi momentum and the baryonic density that are, respectively, given by

$$\rho_i = \frac{\gamma k_{Fi}^3}{6\pi^2}, \tag{5}$$

and

$$\rho_b = \frac{1}{3} \sum_i \rho_i. \tag{6}$$

With regard to the thermodynamical consistency of the model, one can verify this characteristic by different means. The first verification concerns to the condition

$$\Delta = P - \rho_b^2 \frac{d}{d\rho_b} \left(\frac{\mathcal{E}}{\rho_b} \right) = 0. \tag{7}$$

Any consistent thermodynamic model must ensure that $\Delta = 0$ or, in other words, the pressure at the minimum energy per baryon must be zero. A second verification that can be done is through the Euler relation given by

$$P + \mathcal{E} = \sum_i \mu_i \rho_i. \tag{8}$$

Finally, the third option is to analyze the derivative of $-\Omega_0$ with respect to μ_i^* as presented by

$$\rho_i = -\frac{\partial \Omega_0}{\partial \mu_i^*}, \tag{9}$$

where the comparison with the particle number density in Eq. (5) results in an equivalence. These procedures leads us to conclude that all equations of the model are consistent with the ones from fundamental thermodynamics, regardless the choice of the quark mass scaling, such as the ones from [37–40].

Following up on this, for the EQP model the quark masses is constructed as being density dependent as follows:

$$m_i = m_{i0} + m_I = m_{i0} + \frac{D}{\rho_b^{1/3}} + C\rho_b^{1/3}, \tag{10}$$

where m_{i0} is the current mass of the quark i. The interaction effects between the quarks are contained in the parameters C and D, which are chosen from a stability window which will be described later. When working with compact objects, there is an interest of achieving higher stellar masses in order to satisfy the observational constraints. For this reason, the parameter C plays an import role highlighting the necessity of incorporating this parameter into the mass scaling derived from [33] and presented in Eq. (10).

B. Stellar matter

Given the interest in studying compact objects it is necessary to establish the conditions for the matter

present in its interior. At zero temperature and high density regime, stellar matter in pure quark or hybrid stars [41–48] can be described by effective quark models.

The most powerful mechanism of neutrino emission in stars is the Urca process [49, 50], responsible for their cooling since in this process stars lose a significant amount of thermal energy. The rate of neutrino emission influences how quickly the star cools down from its initial high temperature. After neutrinos are emitted from the star, its internal conditions undergoes through some changes, where the beta equilibrium takes place. This condition is given by $\mu_u + \mu_e = \mu_d = \mu_s$ in quark stars, which are the chemical potentials of the particles involved. In therms of the previously discussed model, this relation can be written as $\mu_u^* + \mu_e = \mu_d^* = \mu_s^*$, where the chemical potentials of the quarks are now the effective ones. The electron (e) does not have an effective chemical potential because its mass is constant. This equilibrium condition ensures that the star remains stable and maintains its composition over cosmic timescales. Furthermore, another condition has to be satisfied in compact stars, namely, the charge neutrality condition, given here by $\frac{2}{3}\rho_u - \frac{1}{3}\rho_d - \frac{1}{3}\rho_s - \rho_e = 0$. These conditions exist due to the presence of leptons (electrons in this case), where weak interactions happen such as $d, s \leftrightarrow u + e + \bar{\nu}_e$. Because of the electrons presence, stellar matter is described by the sum of quarks and electrons contribution. Considering the (massless) electrons contribution, the total energy density and pressure of the part of the system composed by "visible" matter are

$$\mathcal{E}_{\text{vis}} = \mathcal{E} + \frac{\mu_e^4}{4\pi^2} \tag{11}$$

and

$$P_{\text{vis}} = P + \frac{\mu_e^4}{12\pi^2}, \tag{12}$$

respectively, with $\mu_e = (3\pi^2 \rho_e)^{1/3}$.

C. Stability window

For the discussion of strange quark matter (SQM) in the context of quark stars, one has to consider the Bodmer-Witten hypothesis [3, 4]. It suggests that under certain conditions, such as at high densities or pressures, SQM may be the true ground state of matter rather than normal nuclear matter. Therefore, in order to establish the stability of SQM we need to investigate it against nuclear matter, which can be done through evaluating the minimum of the energy per baryon, $(E/A)_{\text{min}}$. This evaluation is then classified as follows: (i) SQM is stable when the minimum of the energy per baryon is lower than the binding energy of ^{56}Fe (because it is the heaviest stable nucleus found in nature), i.e., $(E/A)_{\text{min}} \leqslant 930$ MeV; (ii) SQM is considered to be meta-stable when the minimum of the energy per baryon is higher than 930 MeV

and lower than 939 MeV, which is the nucleon mass, i.e., 930 MeV $< (E/A)_{\text{min}} \leqslant 939$ MeV; (iii) SQM is unstable only if the minimum of the energy per baryon is higher than 939 MeV, i.e, $(E/A)_{\text{min}} > 939$ MeV. In the case of stellar matter, we have $E/A = \mathcal{E}_{\text{vis}}/\rho_b$.

With the minimum of the energy per baryon in hand, it is possible to construct what is called the stability window for a large set of values for the C and $\sqrt{D}$ parameters of the EQM model. This analysis is depicted in Fig. 1. In the figure we observe different regions of stabil-
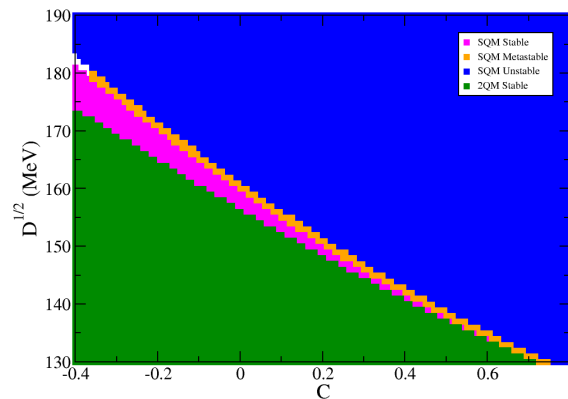

FIG. 1. Stability window for stellar matter predicted by EQP model.

ity for SQM. The pink one corresponds to the absolutely stable state of SQM, which is our area of interest. Below this area we find the green region where two-flavor quark matter (2QM) is stable and where the SQM is forbidden to happen. In the orange region the metastable state of SQM is expected to occur, and in blue we have the unstable SQM. It is important to mention that this analysis takes in consideration the data provided by PDG [51] regarding the ranges for the current quark masses, $m_{u0} = 2.16^{+0.49}_{-0.26}$, $m_{d0} = 4.67^{+0.48}_{-0.17}$ MeV and $m_{s0} = 93.4^{+8.6}_{-3.4}$ MeV. For stellar matter the chosen values are $m_{u0} = 2.16$ MeV , $m_{d0} = 5.15$ MeV, and $m_{s0} = 90$ MeV. For the pair (C, D) we take $C = 0.81$ and $D^{1/2} = 127$ MeV, since it produces more massive stars when only quark matter is considered.

D. Polyakov equiparticle model

The Polyakov equiparticle (PEQP) model was proposed in [34, 52] to study the confinement/deconfinement phase transition, possible to happen inside strange stars. In that article, some of us perform a few modifications in the original EQP model, which will be briefly described in this section. In this improved model, gluons and its corresponding strong interaction dynamics is phenomenologically described by the traced Polyakov loop, Φ. When $\Phi = 0$, the quarks are confined and with $\Phi \to 1$ they achieve the deconfined phase. In the

NJL model [53–58], this quantity was introduced, at finite temperature [59], to generate the so-called Polyakov-Nambu-Jona-Lasinio (PNJL) model [60–66]. At first, the PNJL model loses its characteristics of describing the confinement/deconfinement phase transition at $T = 0$, but in [67] the authors were able to solve this problem by taking the $b_2(T)$ function, present in the Polyakov potential, and modifying it to become a function that is also dependent on the quark density. Later on, the PNJL model suffered another improvement done in [68–70], where the motivation was to ensure that the coupling constants would vanish at the deconfinement phase, i.e. at $\Phi = 1$.

All these observations concerning the improvement of the original NJL model were also implemented in the EQP model. More specifically, the parameters C and D were modified as follows, $C \rightarrow C'(C, \Phi) = C(1 - \Phi^2)$, and $D \rightarrow D'(D, \Phi) = D(1 - \Phi^2)$, which lead us to the a new equation for the quark masses,

$$m_i(\rho_b, \Phi) = m_{i0} + \frac{D(1 - \Phi^2)}{\rho_b^{1/3}} + C(1 - \Phi^2)\rho_b^{1/3}, \quad (13)$$

i.e., now m_i is also a function of ρ_b and Φ as well. For the equations of state, energy density and pressure respectively, we have that $\mathcal{E}_{\mathrm{PEQP}} = \mathcal{E}_{\mathrm{EQP}} + \mathcal{U}_0(\Phi)$ and $P_{\mathrm{PEQP}} = P_{\mathrm{EQP}} - \mathcal{U}_0(\Phi)$ where $\mathcal{U}_0(\Phi)$ is included to ensure $\Phi \neq 0$ solutions and also to limit Φ in the physical range of $0 \leqslant \Phi \leqslant 1$, according to the findings of [68, 69] (we also consider that $\Phi = \Phi^*$). This term is given as $\mathcal{U}_0(\Phi) = a_3 T_0^4 \ln(1 - 6\Phi^2 + 8\Phi^3 - 3\Phi^4)$, with a_3 being a dimensionless free parameter, and $T_0 =$ the transition temperature for the pure gauge system. Notice that if we take $a_3 = 0$, the original EQP model is restored, since this leads to $U_0 = 0$ and, consequently, to $\Phi = 0$, $C' = C$, and $D' = D$. The PEQM model was only introduced here to acknowledge that this model is being studied to explain different physical phenomena in quark matter, but our choice in the present work is to study dark matter inside strange stars by using the original EQP model, i.e., by taking, for the sake of simplicity, $a_3 = 0$.

III. DARK MATTER MODELS

With regard to the dark sector of our approach, we choose to investigate the capability of the DM model in satisfying the recent astrophysical constraints when admixed to the previously described quark matter, by implementing a fermionic and a bosonic model. Concerning the first one, we adopt, as starting point, a Lagrangian density presenting a kinetic term (Dirac Lagrangian density) of a single fermionic component, along with a vector meson coupled to the Dirac spinor. The full expression is given by [71–73]

$$\mathcal{L}_{\mathrm{FDM}} = \bar{\chi}\left[\gamma_\mu(i\partial^\mu - g_V V^\mu) - m_\chi\right]\chi - \frac{1}{4}F_{\mu\nu}F^{\mu\nu}$$
$$+ \frac{1}{2}m_V^2 V_\mu V^\mu, \quad (14)$$

where the strength tensor of the vector meson is $F_{\mu\nu} = \partial_\mu V_\nu - \partial_\nu V_\mu$. The dark fermion mass is m_χ, and m_V is the mass of the dark vector meson. We do not include here the dark scalar meson, as done in [71], in order to simplify the model and avoid one more free parameter to be fixed. Besides that, the main effect for increasing the final compact star mass is due to repulsion interactions. Therefore, the inclusion of a scalar particle would add the attraction to the system and, consequently, a decreasing of the repulsion as a net feature.

In a similar way as done in relativistic hadronic models that present the same mathematical formulation for the Lagrangian density, we employ here the mean field approach in order to compute energy density and pressure of the dark sector of the system. These expressions read

$$\mathcal{E}_{\mathrm{FDM}} = \frac{1}{\pi^2}\int_0^{k_{F\chi}} dk\, k^2(k^2 + m_\chi^2)^{1/2} + \frac{1}{2}C_V^2\rho_\chi^2, \quad (15)$$

$$P_{\mathrm{FDM}} = \frac{1}{3\pi^2}\int_0^{k_{F\chi}} dk\, \frac{k^4}{(k^2 + m_\chi^2)^{1/2}} + \frac{1}{2}C_V^2\rho_\chi^2, \quad (16)$$

with $C_V = g_V/m_V$ and $\rho_\chi = k_{F\chi}^3/(3\pi^2)$. The Fermi momentum of the dark particle is $k_{F\chi}$. Fermionic self-interacting dark matter models coupled to hadronic matter were used in the description of neutron stars with DM content, as the reader can find in [74], for instance.

Despite efforts dedicated to the direct and indirect detection methods for dark matter in the last years [75], the true nature of DM particle is still not well established. This is the origin of the many possible candidates studied over the years, as the weakly interacting massive particles, gravitinos, axinos, axions, sterile neutrinos, WIMPzillas, supersymmetric Q-balls, and mirror matter [76, 77]. Among these options, both fermionic and bosonic dark particles are considered. In order to take into account the latter ones, we assume the bosonic asymmetric dark matter model proposed in [78] and explored in details in [79]. After neglecting interactions between the dark boson with visible matter, and approximating the spacetime to be flat, the Lagrangian density for the model reads

$$\mathcal{L}_{\mathrm{BDM}} = -\sqrt{-g}\left(D_\mu^*\sigma^* D^\mu\sigma - m_\sigma^2\sigma^*\sigma - \frac{1}{2}m_\phi^2\phi_\mu\phi^\mu\right.$$
$$\left. - \frac{1}{4}Z_{\mu\nu}Z^{\mu\nu}\right) \quad (17)$$

where $D_\mu = \partial_\mu + ig_\sigma\phi_\mu$, g_σ is the interaction strength of the dark scalar complex field σ with the dark vector field ϕ^μ, $Z_{\mu\nu} = \partial_\mu\phi_\nu - \partial_\nu\phi_\mu$, and g is the determinant of the metric. The masses of the dark scalar and dark

vector fields are m_σ and m_ϕ, respectively. Usual quantum field theory techniques, along with the mean field approximation, lead to the following energy-momentum tensor

$$T_{\mu\nu} = 2D_\mu^* \sigma^* D_\nu \sigma - g_{\mu\nu} \left(D_\rho^* \sigma^* D^\rho \sigma + m_\sigma^2 \sigma^* \sigma \right) + m_\sigma^2 \left(\phi_\mu \phi_\nu - \frac{1}{2} g_{\mu\nu} \phi_\rho \phi^\rho \right), \qquad (18)$$

that is used to find the equations of state for the bosonic DM model given by

$$\mathcal{E}_{\text{BDM}} = m_\sigma \rho_\sigma + \frac{1}{2} C_{\sigma\phi}^2 \rho_\sigma^2, \qquad (19)$$

$$P_{\text{BDM}} = \frac{1}{2} C_{\sigma\phi}^2 \rho_\sigma^2, \qquad (20)$$

with $C_{\sigma\phi} = g_\sigma/m_\phi$. The DM density ρ_σ relates to the zero component of the vector field ϕ_0, and with the scalar field and its conjugate through $\phi_0 = (g_\sigma/m_\phi^2)\rho_\sigma$, and $\rho_\sigma = 2m_\sigma \sigma^* \sigma$, respectively. Detailed derivation of these expressions can be found in [79]. We also address the reader to [80] for a deeper study of scalar fields, in general, in the gravitational context. Other similar bosonic DM models coupled to luminous matter, studying neutron stars in particular, were analyzed in [81, 82].

In the analysis of bosonic DM inside compact stars, it is important to emphasize that Black holes can be formed when the Chandrasekhar limit is achieved [83]. In the case of fermionic matter in ground state, the Pauli exclusion principle helps balancing gravity since degeneracy pressure is present. For bosonic systems, on the other hand, the lack of Fermi pressure sets this limit to a smaller value. However, it can be increased due to repulsive interactions like the one included in Eq. (17). In order to satisfy this condition, we restrict the values of m_σ and $C_{\sigma\phi}$ to 10^{-2} MeV $\leqslant m_\sigma \leqslant 10^8$ MeV and 10^{-2} MeV$^{-1} \leqslant C_{\sigma\phi} \leqslant 10^3$ MeV^{-1}, respectively, in agreement to the findings of [79].

IV. STRANGE STARS ADMIXED WITH DARK MATTER

For the construction of strange stars through the EQP model admixed with fermionic or bosonic dark matter, all of them previously discussed, we consider the inter-fluid interaction uniquely coming from gravitational effects. For this purpose, the two-fluid formalism is a suitable treatment. In this approach, each fluid satisfies conservation of energy-momentum separately, that is equivalent to have $P(r) = P_{\text{vis}}(r) + P_{\text{DM}}(r)$ and $\mathcal{E}(r) = \mathcal{E}_{\text{vis}}(r) + \mathcal{E}_{\text{DM}}(r)$, with r being the radial coordinate from the center of the star. This consideration leads to the

following differential TOV equations to be solved,

$$\frac{dP_{\text{vis}}(r)}{dr} = -\frac{\left[\mathcal{E}_{\text{vis}}(r) + P_{\text{vis}}(r)\right]\left[m(r) + 4\pi r^3 P(r)\right]}{r\left[r - 2m(r)\right]}, \qquad (21)$$

$$\frac{dP_{\text{DM}}(r)}{dr} = -\frac{\left[\mathcal{E}_{\text{DM}}(r) + P_{\text{DM}}(r)\right]\left[m(r) + 4\pi r^3 P(r)\right]}{r\left[r - 2m(r)\right]}, \qquad (22)$$

$$\frac{dm_{\text{vis}}(r)}{dr} = 4\pi r^2 \mathcal{E}_{\text{vis}}(r), \qquad (23)$$

$$\frac{dm_{\text{DM}}(r)}{dr} = 4\pi r^2 \mathcal{E}_{\text{DM}}(r), \qquad (24)$$

where $m(r) = m_{\text{vis}}(r) + m_{\text{DM}}(r)$ is the total mass contained in the sphere of radius r. The visible matter mass is $m_{\text{vis}}(r)$, and the dark matter mass is $m_{\text{DM}}(r)$. In these equations, one has DM = FDM (BDM) for fermionic (bosonic) dark matter. This set of coupled equations can be obtained from the stationary condition of the star mass. For a detailed derivation, we address the reader to the appendix of [71].

Technically, the procedure adopted to solve Eqs. (21)-(24) is the following. First we define the four initial conditions as $m_{\text{vis}}(0) = m_{\text{DM}}(0) = 0$, $P_{\text{vis}}(0) = P_{\text{vis}}^c$, and $P_{\text{DM}}(0) = P_{\text{DM}}^c$, where P_{vis}^c and P_{DM}^c are the central pressures related to visible and dark matter, respectively, given by the equations of state presented in the previous sections. Then, for each set of initial conditions we use the fourth order Runge–Kutta method in order to obtain pressures and masses as functions of r. The radii R_{vis} and R_{DM} are defined as being the quantities that lead to $P_{\text{vis}}(R_{\text{vis}})/P_{\text{vis}}^c = 0$ and $P_{\text{DM}}(R_{\text{DM}})/P_{\text{DM}}^c = 0$, within a certain tolerance. These radii are also useful to determine $M_{\text{vis}} \equiv m_{\text{vis}}(R_{\text{vis}})$, and $M_{\text{DM}} \equiv m_{\text{DM}}(R_{\text{DM}})$. Therefore, the total mass of the respective star is $M = M_{\text{vis}} + M_{\text{DM}}$, and its radius is $R = R_{\text{vis}}$ if $R_{\text{vis}} > R_{\text{DM}}$, or $R = R_{\text{DM}}$ if $R_{\text{DM}} > R_{\text{vis}}$. This latter case identifies dark matter halo configurations for the star of mass M and radius R. This mechanism is repeated for each point of the input equations of state, with the final collected pairs (M, R) giving rise to the mass-radius diagram.

Here we impose that every star present a certain fraction of dark matter in its composition, i.e., a fixed value of $F_{\text{DM}} = M_{\text{DM}}/M$. In order to satisfy this restriction, we proceed as follows. First one needs to construct all the inputs for the TOV equations, namely, P_{vis}^c, $\mathcal{E}_{\text{vis}}^c$, P_{DM}^c and $\mathcal{E}_{\text{DM}}^c$ (despite not directly used as initial conditions, the energy densities have also to be furnished since their relationships with the pressures are used to replace $\mathcal{E}$'s by P's in the TOV equations). The visible matter equation of state (EOS) is straightforward, directly evaluated from Eqs. (11)-(12). For both DM models, fermionic and bosonic, we connect them with the EQP model by imposing that $\mathcal{E}_{\text{DM}} = f\mathcal{E}_{\text{vis}}$ where the energy density fraction, f, is a constant [71]. In the case of the bosonic DM model, this leads to an analytical expression for the dark boson

density,

$$\rho_\sigma = \frac{m_\sigma}{C_{\sigma\phi}^2} \left(\sqrt{1 + \frac{2C_{\sigma\phi}^2}{m_\sigma^2} f\mathcal{E}_{\text{vis}}} - 1 \right), \qquad (25)$$

and, consequently, to a direct relation between dark pressure and quark energy density given by

$$P_{\text{BDM}} = \frac{m_\sigma^2}{2C_{\sigma\phi}^2} \left(\sqrt{1 + \frac{2C_{\sigma\phi}^2}{m_\sigma^2} f\mathcal{E}_{\text{vis}}} - 1 \right)^2. \qquad (26)$$

For the fermionic dark matter case, on the other hand, there are not simple expressions relating the equations of states of quark and dark matter. The free parameters of the dark sector used here are $m_\sigma = 15$ GeV [79], $C_{\sigma\phi} = 0.1$ MeV^{-1} [79], $m_\chi = 1.9$ GeV, and $C_V = 3.26$ fm. The last two values, inside the ranges 0.5 GeV $\leqslant m_\chi \leqslant 4.5$ GeV [84] and 0.1 fm $\leqslant C_V \leqslant 5$ fm [71], were taken from [73]. As an illustration, we display BDM and FDM cases in Fig. 2 for fixed f. Notice that for the chosen set
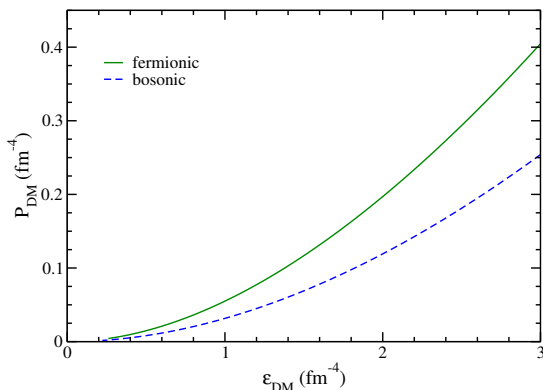

FIG. 2. Dark matter pressure as a function of its respective energy density. Fermionic and bosonic cases.

of parameters the fermionic EOS is stiffer in comparison with the BDM one, as expected.

Since the connection $\mathcal{E}_{\text{DM}} = f\mathcal{E}_{\text{vis}}$ is established, we solve the two-fluid TOV equations for huge set of values for f. For each solution related to a particular f, we evaluate F_{DM} and select, among all the solutions, only the (M, R) pairs that satisfy the particular value of F_{DM} chosen. The final result consists in a mass-radius diagram representing quark stars, each one of them admixed with a fixed fraction of dark matter.

As a remark, we emphasize that the two-fluid approach requires a detailed analysis on the stability of the final compact quark-DM star obtained, as the reader can verify in [85, 86]. In a one fluid system, the search for stable configurations consists in investigating the response of the star to radial oscillations in a Sturm-Liouville problem for the relative radial displacement and the pressure perturbation, both quantities depending on time through $e^{i\omega t}$ with ω being the eigenfrequency. Basically, the solutions of the new differential equations emerged from

this investigation determines that stable stars are those in which $\omega^2 > 0$. Solutions presenting $\omega^2 < 0$ correspond to an exponential increasing of the perturbation, leading, consequently, to the collapse of the compact star. In the case of homogeneous stars, i.e., those presenting just one phase, the location of the last stable star ($\omega = 0$) coincides with the maximum mass point in the mass-radius diagram, equivalent to the point in which $\partial M/\partial\mathcal{E}^c = 0$.

In the case of the two-fluid method, the generalization determines that at the onset of unstable configurations the number of visible (N_{vis}) and dark (N_{DM}) particles are stationary under variations of $\mathcal{E}_{\text{vis}}^c$ and $\mathcal{E}_{\text{DM}}^c$. As pointed out in [85, 86], it is analogous to diagonalize the matrix $\partial N_i/\partial\mathcal{E}_j^c$ (i, j=VIS, DM) with the aim of searching for its associated eingenvalues, claimed to be both positive for stable stars configurations. However, as discussed in [87], there is an indication that DM models presenting central pressures in the range of $P_{\text{DM}}^c \lesssim 5.1$ fm^{-4} generate stars in a stable region. Both DM models used in this work, bosonic and fermionic ones, are in agreement with this constraint. Furthermore, the authors of [88, 89] have used in their calculations, based on previous studies [90, 91], that the maxima of the fixed F_{DM} curves represent the last stable stars in the mass-radius diagram, as it is in the case of one fluid systems. In our study we adopt the same procedure and exclude points beyond the maximum one. The final mass-radius diagrams for both models described here are shown in Fig. 3.

From this figure, one can verify that the maximum mass (M_{max}) of each diagram decreases as the mass fraction increases. This is a result compatible with previous studies that predict such a reduction in stars configurations in which a DM core is observed [78, 93–96]. As a illustration, we plot M_{max} versus F_{DM} for both cases (BDM and FDM models) in Fig. 4. It is worth noticing the strong linear relation between the maximum mass and the dark matter content. As a consequence, one has a constant decreasing rate of M_{max} as a function of F_{DM}. Such behavior is hard to be predicted before calculations due to the nontrivial structure of both, the two-fluid equations and the equations of state used as input, in our case, the EQP model in the visible sector, and the fermionic/bosonic models in the description of dark matter. We also furnish the slope of the linear fitting obtained, namely, -0.0343 (-0.315) for bosonic (fermionic) model. Notice that both are very similar. Furthermore, these values are very close to -0.0362, result found in [97] in a study performed with a completely different quark model in the ordinary matter sector: the MIT bag model. For the dark sector, they have used a model made up of fermionic particles of mass 100 GeV, number more than 50 times greater than the value used in the current work for the FDM model. This result maybe indicates a possible universality in the (linear) decreasing behavior of the maximum mass in quark models admixed with dark matter.

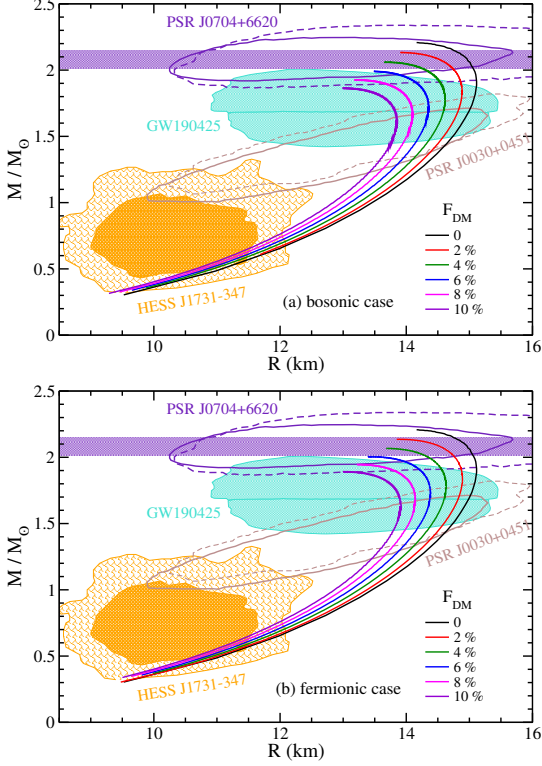In Fig. 4 we can also verify that the FDM model produces maximum masses slightly greater than the ones

FIG. 3. Mass-radius relations for different fractions of dark matter in each strange stars. Results for (a) bosonic and (b) fermionic cases. The contours are related to data from the NICER mission, namely, PSR J0030+0451 [11, 12] and PSR J0740+6620 [13, 14], and the GW190425 event [10], all of them at 90% credible level. The violet horizontal lines are also related to the PSR J0740+6620 pulsar [92].
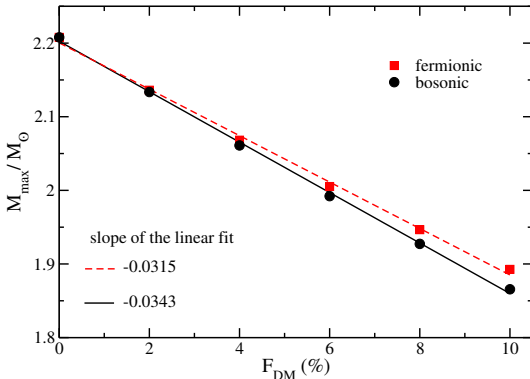

FIG. 4. Maximum total mass versus mass fraction for the strange-DM stars presented in Fig. 3.

generated from the BDM model, feature observed for the range of parameters investigated in our analysis. It

suggests that DM equations of state are stiffer for the fermionic case with fixed dark matter content in comparison with the bosonic description of the dark sector as, indeed, we already shown in Fig. 2. This particular figure was plotted for a fixed f, but since the equations of state given as input are the same, the curves produced for a fixed value of F_{DM} are also the same.

Still regarding the features related to Fig. 3, we emphasize that the difference between the entire mass-radius curves generated from the quark-FDM approach and from the quark-BDM one are very small. We assign this effect to the dominance of the effective quark model over both, bosonic and fermionic DM models used in the analysis. In order to illustrate this statement, we display in Figs. 5 the profiles of the same star constructed by using both BDM and FDM models, with $M = 1.81 M_\odot$ and 10% of dark matter in its composition.
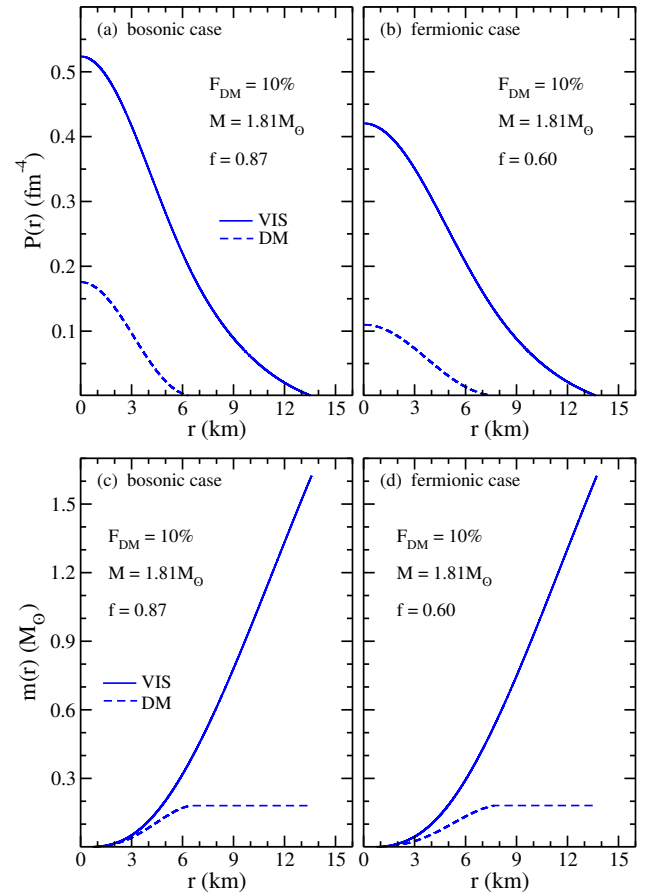

FIG. 5. Pressure (panels a and b) and enclosed mass (panels c and d) as functions of radial coordinate for a mass fraction equal to 10% and total stellar mass of $M = 1.81 M_\odot$. Full (dashed) lines: visible (dark) matter. For the bosonic (fermionic) case in panel a (b), the energy density fraction is $f = 0.87$ (0.6).

Notice from this example that the radius of the star is $R = R_{vis} \simeq 13.6$ (13.7) km, since $R_{vis} > R_{DM}$ in this case, by using the bosonic (fermionic) model in the dark

sector. The main modification caused by the interchange of the DM model is the central pressure (at $r = 0$) in both sectors. Nevertheless, R_{vis} is still pratically equal for both models and determines the radius of the final star, according to the criterion used to define this quantity (R corresponds to the outermost radius between R_{vis} and R_{DM}). However, the situation is not the same for stars in which a DM halo is formed around it. We can verify such an effect for the case of $M = 1.86 M_\odot$ and $F_{DM} = 10\%$, depicted in Fig. 6, for the strange star constructed with inclusion of bosonic dark matter in particular. In this figure we present two parametriza-
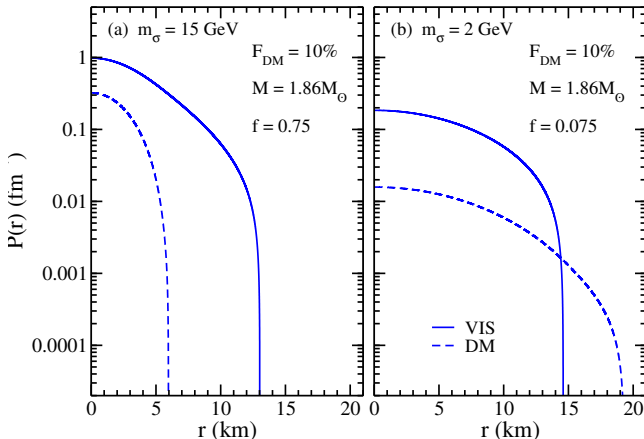

FIG. 6. Pressure as a function of radial coordinate for a mass fraction equal to 10% and total stellar mass of $M = 1.86 M_\odot$. Full (dashed) lines: visible (dark) matter. Strange star admixed with bosonic dark matter with $m_\sigma = 15$ GeV (panel a) and $m_\sigma = 2$ GeV (panel b).

tions of the BDM model, specifically with different values of the dark boson mass, namely, $m_\sigma = 15$ GeV (standard value previously used) and $m_\sigma = 2$ GeV. Notice that the decrease of the dark particle mass induces the situation of $R_{DM} > R_{vis}$ producing, consequently, the formation of a DM halo. In this case, the radius of the final star changes from $R = R_{vis} \simeq 13$ km to $R = R_{DM} \simeq 19$ km. Since fermionic and bosonic models generate similar mass-radius diagrams for $m_\sigma = 15$ GeV and $m_\chi = 1.9$ GeV, the decrease of m_σ will produce a more pronounced difference between the diagrams obtained from FDM model with $m_\chi = 1.9$ GeV in comparison with the ones determined from BDM model with $m_\sigma = 2$ GeV, due to the emergence of DM halos in the latter system. These features are compatible with studies presented, for instance, in [96] where the authors used the two-fluid approach with bosonic DM, and in [98] where a fermionic DM model is applied in the description of stellar matter. In these works, the DM halo formation is observed when the dark particle (bosons or fermions) are decreased. In particular, since they treat neutron stars, hadronic models are used in the visible matter sector. In our work, on the other hand, strange stars are studied

but the same effect is exhibited as well.

Last but not least, we remark the compatibility of our results with the recent observational astrophysical data provided by the NICER mission regarding the millisecond pulsars PSR J0030+0451 [11, 12] and PSR J0740+6620 [13, 14], and with data from the gravitational wave event GW190425 [10] analyzed by LIGO and Virgo Collaboration. The same is observed with the PSR J0740+6620 data extracted from [92], corresponding to $M = (2.08 \pm 0.07) M_\odot$ at 68.3% of credible level, and with the compact star named as HESS J1731-347 [16]. It points out to possible scenarios in which strange stars can admit dark matter in its interior.

V. SUMMARY AND CONCLUDING REMARKS

In this work we have investigated the possible scenarios concerning the existence of strange quark stars with dark matter in its composition. The description of ordinary strongly interacting matter was made through the so called equiparticle (EQP) model [33, 35], in which the constituent quark masses (u, d, s quarks) are affected by the medium by means of suitable baryonic density dependent functions. The parameters present in these functions were chosen from the analysis of the stellar matter stability window, by imposing parametrizations with lower energy per baryon in comparison with the iron nuclei. Similar studies were performed in [87, 97], but based on versions of the MIT bag model in the description of the "visible" sector of the system. An improved version of the EQP model was proposed in [34, 52], where the Polyakov loop was included with the aim of representing the gluonic dynamics of the strong interaction. As a consequence, the new model was verified to be able of describing quark matter (first order) transition from confined to deconfined phase at zero-temperature regime.

The dark matter part of the system was studied from two different models, namely, a fermionic and a bosonic one. The former was described by a Lagrangian density in which the dark spinor feels a repulsive interaction coming from a dark vector field. The full equations of state only depend on two free parameters: the dark fermion mass (m_χ), and the ratio between the strength of the vector interaction (g_V) and the vector field mass (m_V). We consider these quantities inside the ranges of 0.5 GeV $\leqslant m_\chi \leqslant$ 4.5 GeV [84] and 0.1 fm $\leqslant C_V = g_V/m_V \leqslant$ 5 fm [71]. With regard to the bosonic model, we consider a version where we neglect interactions between the dark boson and the quarks. As in the fermionic case, we also take into account a vector interaction, in this case crucial in order to avoid the collapse of the resulting star due to the absence of degeneracy pressure. The final equations for energy density and pressure are derived and, once again, two free parameters are needed to completely determine the model: the dark scalar mass (m_σ) and $C_{\sigma\phi} = g_\sigma/m_\sigma$, where g_σ is the interaction strength of the dark scalar

complex field with the dark vector field. Here we take values compatible with 10^{-2} MeV $\leqslant m_\sigma \leqslant 10^8$ MeV and 10^{-2} MeV$^{-1} \leqslant C_{\sigma\phi} \leqslant 10^3$ MeV^{-1} [79].

Since luminous and dark matter models are defined, we let both sectors interact only by gravity through a two-fluid approach. Our results point out to strange stars admixed with dark matter, with fixed dark matter fraction, as a possible scenario in agreement with astrophysical data coming from the massive millisecond pulsars PSR J0030+0451 [11, 12] and PSR J0740+6620 [13, 14], the NASA's Neutron star Interior Composition Explorer (NICER) x-ray telescope, and the compact star

named as HESS J1731-347 [16].

[1] D. D. Ivanenko and D. F. Kurdgelaidze, Astrophysics **1**, 251 (1965).

[2] D. D. Ivanenko and D. F. Kurdgelaidze, Sov. Phys. J. **13**, 1015 (1970).

[3] A. R. Bodmer, Phys. Rev. D **4**, 1601 (1971).

[4] E. Witten, Phys. Rev. D **30**, 272 (1984).

[5] E. Annala, T. Gorda, A. Kurkela, J. Nättilä, and A. Vuorinen, Nature Physics **16**, 907 (2020).

[6] E. Annala, T. Gorda, J. Hirvonen, O. Komoltsev, A. Kurkela, J. Nättilä, and A. Vuorinen, Nature Communications **14**, 8451 (2023).

[7] B. P. Abbott, R. Abbott, T. D. Abbott, F. Acernese, K. Ackley, C. Adams, et al., The Astrophysical Journal Letters **848**, L12 (2017).

[8] B. P. Abbott, R. Abbott, T. D. Abbott, F. Acernese, K. Ackley, et al. (LIGO Scientific Collaboration and Virgo Collaboration), Phys. Rev. Lett. **119**, 161101 (2017).

[9] B. P. Abbott, R. Abbott, T. D. Abbott, F. Acernese, Ackley, et al. (The LIGO Scientific Collaboration and the Virgo Collaboration), Phys. Rev. Lett. **121**, 161101 (2018).

[10] B. P. Abbott, R. Abbott, T. D. Abbott, S. Abraham, F. Acernese, et al., The Astrophysical Journal Letters **892**, L3 (2020).

[11] T. E. Riley, A. L. Watts, S. Bogdanov, P. S. Ray, et al., The Astrophysical Journal Letters **887**, L21 (2019).

[12] M. C. Miller, F. K. Lamb, A. J. Dittmann, S. Bogdanov, et al., The Astrophysical Journal Letters **887**, L24 (2019).

[13] T. E. Riley, A. L. Watts, P. S. Ray, S. Bogdanov, et al., The Astrophysical Journal Letters **918**, L27 (2021).

[14] M. C. Miller, F. K. Lamb, A. J. Dittmann, S. Bogdanov, et al., The Astrophysical Journal Letters **918**, L28 (2021).

[15] K. Gendreau and Z. Arzoumanian, Nature Astronomy **1**, 895 (2017).

[16] V. Doroshenko, V. Suleimanov, G. Pühlhofer, and A. Santangelo, Nature Astronomy **6**, 1444 (2022).

[17] G. Bertone and D. Hooper, Rev. Mod. Phys. **90**, 045002 (2018).

[18] A. Arbey and F. Mahmoudi, Progress in Particle and Nuclear Physics **119**, 103865 (2021).

[19] P. Salucci, The Astronomy and Astrophysics Review **27**, 2 (2019).

[20] L. V. E. Koopmans and T. Treu, The Astrophysical Journal **583**, 606 (2003).

[21] R. Massey, T. Kitching, and J. Richard, Reports on Progress in Physics **73**, 086901 (2010).

[22] J. A. Adams, S. Sarkar, and D. W. Sciama, Monthly Notices of the Royal Astronomical Society **301**, 210 (1998).

[23] E. Pierpaoli, Phys. Rev. Lett. **92**, 031301 (2004).

[24] N. Padmanabhan and D. P. Finkbeiner, Phys. Rev. D **72**, 023508 (2005).

[25] Planck Collaboration, Aghanim, N., Arnaud, M., Ashdown, M., Aumont, J., Baccigalupi, C., Banday, A. J., Barreiro, R. B., Bartlett, J. G., Bartolo, N., Battaner, E., Benabed, K., Benoît, A., Benoit-Lévy, A., Bernard, J.-P., Bersanelli, M., Bielewicz, P., et al., Astronomy and Astrophysics **594**, A11 (2016).

[26] W. Hu and S. Dodelson, Annual Review of Astronomy and Astrophysics **40**, 171 (2002).

[27] W. Hu, N. Sugiyama, and J. Silk, Nature (London) **386**, 37 (1997), arXiv:astro-ph/9504057 [astro-ph].

[28] A. Issifu and T. Frederico, Hot quark matter and merger remnants (2024), arXiv:2401.08551 [hep-ph].

[29] X. J. Wen, X. H. Zhong, G. X. Peng, P. N. Shen, and P. Z. Ning, Phys. Rev. C **72**, 015204 (2005).

[30] A. Issifu, F. M. da Silva, and D. P. Menezes, European Physical Journal C **84**, 463 (2024).

[31] H.-M. Chen, C.-J. Xia, and G.-X. Peng, Phys. Rev. D **105**, 014011 (2022).

[32] A. Issifu, F. M. da Silva, L. C. N. Santos, D. P. Menezes, and T. Frederico, Strongly interacting quark matter in massive quark stars (2024), arXiv:2408.15889 [nucl-th].

[33] C. J. Xia, G. X. Peng, S. W. Chen, Z. Y. Lu, and J. F. Xu, Phys. Rev. D **89**, 105027 (2014).

[34] I. Marzola, S. B. Duarte, C. H. Lenzi, and O. Lourenço, Phys. Rev. D **108**, 083006 (2023).

[35] B. C. Backes, E. Hafemann, I. Marzola, and D. P. Menezes, J. Phys. G **48**, 055104 (2021).

[36] G. X. Peng, A. Li, and U. Lombardo, Phys. Rev. C **77**, 065807 (2008).

[37] G. X. Peng, H. C. Chiang, B. S. Zou, P. Z. Ning, and S. J. Luo, Phys. Rev. C **62**, 025801 (2000).

[38] G. N. WFowler, S. Raha, and R. M. Weiner, Z. Phys. C **9**, 1431 (1981).

[39] S. Chakrabarty, Phys. Rev. D **43**, 627 (1991).

[40] Z. Xiaoping, L. Xuewen, K. Miao, and Y. Shuhua, Phys. Rev. C **70**, 015803 (2004).

[41] K. Schertler, S. Leupold, and J. Schaffner-Bielich, Phys. Rev. C **60**, 025801 (1999).

[42] I. F. Ranea-Sandoval, M. G. Orsaria, G. Malfatti, D. Curin, M. Mariani, G. A. Contrera, and O. M. Guilera, Symmetry **11**, 10.3390/sym11030425 (2019).

[43] M. Hanauske, L. M. Satarov, I. N. Mishustin, H. Stöcker, and W. Greiner, Phys. Rev. D **64**, 043005 (2001).

[44] D. P. Menezes, C. Providência, and D. B. Melrose, J. Phys. G: Nucl. Part. Phys. **32**, 1081 (2006).

[45] C. H. Lenzi, A. S. Schneider, C. Providência, and R. M. Marinho, Phys. Rev. C **82**, 015809 (2010).

[46] A. Drago and G. Pagliara, Phys. Rev. D **102**, 063003 (2020).

[47] R. C. Pereira, P. Costa, and C. m. c. Providência, Phys. Rev. D **94**, 094001 (2016).

[48] M. Ferreira, R. C. Pereira, and C. m. c. Providência, Phys. Rev. D **102**, 083030 (2020).

[49] J. M. Lattimer, C. J. Pethick, M. Prakash, and P. Haensel, Phys. Rev. Lett. **66**, 2701 (1991).

[50] D. Yakovlev, A. Kaminker, O. Gnedin, and P. Haensel, Physics Reports **354**, 1 (2001).

[51] R. L. Workman and Others (Particle Data Group), PTEP **2022**, 083C01 (2022).

[52] I. Marzola, S. B. Duarte, and O. Lourenço, PoS **XVHadronPhysics**, 065 (2022).

[53] Y. Nambu and G. Jona-Lasinio, Phys. Rev. **122**, 345 (1961).

[54] Y. Nambu and G. Jona-Lasinio, Phys. Rev. **124**, 246 (1961).

[55] S. P. Klevansky, Rev. Mod. Phys. **64**, 649 (1992).

[56] M. Buballa, Physics Reports **407**, 205 (2005).

[57] U. Vogl and W. Weise, Progress in Particle and Nuclear Physics **27**, 195 (1991).

[58] T. Hatsuda and T. Kunihiro, Physics Reports **247**, 221 (1994).

[59] K. Fukushima, Physics Letters B **591**, 277 (2004).

[60] C. Ratti, M. A. Thaler, and W. Weise, Phys. Rev. D **73**, 014019 (2006).

[61] S. Rößner, C. Ratti, and W. Weise, Phys. Rev. D **75**, 034007 (2007).

[62] C. Ratti, S. Rößner, M. Thaler, and W. Weise, The European Physical Journal C **49**, 1434 (2007).

[63] K. Fukushima, Phys. Rev. D **77**, 114028 (2008).

[64] V. A. Dexheimer and S. Schramm, Phys. Rev. C **81**, 045201 (2010).

[65] V. Dexheimer, R. O. Gomes, T. Klähn, S. Han, and M. Salinas, Phys. Rev. C **103**, 025808 (2021).

[66] S. Rößner, Phases of QCD, Ph.D. thesis, Technische Universität München (2009).

[67] O. Ivanytskyi, M. A. Pérez-García, V. Sagun, and C. Albertus, Phys. Rev. D **100**, 103020 (2019).

[68] O. A. Mattos, O. Lourenço, and T. Frederico, J. Phys. Conf. Ser. **1291**, 012031 (2019).

[69] O. A. Mattos, O. Lourenço, and T. Frederico, The European Physical Journal C **81**, 1434 (2021).

[70] O. A. Mattos, T. Frederico, C. H. Lenzi, M. Dutra, and O. Lourenço, Phys. Rev. D **104**, 116001 (2021).

[71] Q.-F. Xiang, W.-Z. Jiang, D.-R. Zhang, and R.-Y. Yang, Phys. Rev. C **89**, 025803 (2014).

[72] A. Das, T. Malik, and A. C. Nayak, Phys. Rev. D **105**, 123034 (2022).

[73] P. Thakur, T. Malik, A. Das, T. K. Jha, and C. m. c. Providência, Phys. Rev. D **109**, 043030 (2024).

[74] M. Mariani, C. Albertus, M. d. R. Alessandroni, M. G. Orsaria, M. A. Pérez-García, and I. F. Ranea-Sandoval, Monthly Notices of the Royal Astronomical Society **527**, 6795 (2024).

[75] D. Bauer, J. Buckley, M. Cahill-Rowley, R. Cotta, A. Drlica-Wagner, J. L. Feng, S. Funk, J. Hewett, D. Hooper, A. Ismail, M. Kaplinghat, A. Kusenko, K. Matchev, D. McKinsey, T. Rizzo, W. Shepherd, T. M. Tait, A. M. Wijangco, and M. Wood, Physics of the Dark Universe **7-8**, 16 (2015).

[76] A. Kusenko and L. J. Rosenberg, Snowmass-2013 cosmic frontier 3 (cf3) working group summary: Non-wimp dark matter (2013), arXiv:1310.8642 [hep-ph].

[77] J. L. Feng, Annual Review of Astronomy and Astrophysics **48**, 495 (2010).

[78] A. E. Nelson, S. Reddy, and D. Zhou, Journal of Cosmology and Astroparticle Physics **2019** (07), 012.

[79] N. Rutherford, G. Raaijmakers, C. Prescod-Weinstein, and A. Watts, Phys. Rev. D **107**, 103051 (2023).

[80] M. Y. Khlopov, B. A. Malomed, and Y. B. Zeldovich, Monthly Notices of the Royal Astronomical Society **215**, 575 (1985).

[81] S. Shakeri and D. R. Karkevandi, Phys. Rev. D **109**, 043029 (2024).

[82] D. Rafiei Karkevandi, M. Shahrbaf, S. Shakeri, and S. Typel, Particles **7**, 201 (2024).

[83] S. D. McDermott, H.-B. Yu, and K. M. Zurek, Phys. Rev. D **85**, 023519 (2012).

[84] X. Calmet and F. Kuipers, Physics Letters B **814**, 136068 (2021).

[85] M. F. Barbat, J. Schaffner-Bielich, and L. Tolos, Phys. Rev. D **110**, 023013 (2024).

[86] M. Hippert, E. Dillingham, H. Tan, D. Curtin, J. Noronha-Hostler, and N. Yunes, Phys. Rev. D **107**, 115028 (2023).

[87] B. Hong and Z. Ren, Phys. Rev. D **110**, 023012 (2024).

[88] H.-M. Liu, J.-B. Wei, Z.-H. Li, G. Burgio, and H.-J. Schulze, Physics of the Dark Universe **42**, 101338 (2023).

[89] H.-M. Liu, J.-B. Wei, Z.-H. Li, G. F. Burgio, H. C. Das, and H.-J. Schulze, Phys. Rev. D **110**, 023024 (2024).

[90] S.-C. Leung, M.-C. Chu, and L.-M. Lin, Phys. Rev. D **85**, 103528 (2012).

[91] K.-L. Leung, M.-c. Chu, and L.-M. Lin, Phys. Rev. D **105**, 123010 (2022).

[92] E. Fonseca, H. T. Cromartie, T. T. Pennucci, P. S. Ray, et al., The Astrophysical Journal Letters **915**, L12 (2021).

[93] J. Ellis, G. Hütsi, K. Kannike, L. Marzola, M. Raidal, and V. Vaskonen, Phys. Rev. D **97**, 123007 (2018).

[94] O. Ivanytskyi, V. Sagun, and I. Lopes, Phys. Rev. D **102**, 063028 (2020).

[95] S.-C. Leung, M.-C. Chu, and L.-M. Lin, Phys. Rev. D **84**, 107301 (2011).

[96] D. Rafiei Karkevandi, S. Shakeri, V. Sagun, and O. Ivanytskyi, Phys. Rev. D **105**, 023001 (2022).

[97] P. Mukhopadhyay and J. Schaffner-Bielich, Phys. Rev. D **93**, 083009 (2016).

[98] P. Routaray, S. R. Mohanty, H. Das, S. Ghosh, P. Kalita, V. Parmar, and B. Kumar, Journal of Cosmology and Astroparticle Physics **2023** (10), 073.